

Determination of the position maximum for electron Compton scattering in electron microscopy

D. S. Su

*Department of Materials Science, Jilin University, Changchun 130021, China
and Fritz-Haber Institut der Max-Planck Gesellschaft, Faradayweg 4-6, D-14195 Berlin, Germany*

P. Schattschneider

*Institut für Angewandte Physik, Technische Universität Wien, Wiedner Hauptstrasse 8-10/137,
A-1040 Vienna, Austria*

E. Zeitler

Fritz-Haber Institut der Max-Planck Gesellschaft, Faradayweg 4-6, D-14195 Berlin, Germany

(Received 29 September 1993)

We study electron Compton scattering with an electron microscope by means of a Castaing-Henry filter. In the electron-spectroscopic-diffraction mode the positions of the Compton maxima in the diffraction plane are determined. We find a nearly constant shift of this position with respect to the value given by $E=q^2/2$. The intensity of Compton-scattered electrons does not peak at the scattering angle predicted by the binary collision mode. The energy dispersion of the Compton profile is well described by $E=q^2/2$.

INTRODUCTION

The combination of the capabilities of an imaging energy filter with the principal operation modes of a transmission electron microscope gives access to many new qualitative and quantitative techniques in electron microscopy.¹ These techniques can be divided into two categories: (1) The filter is used as low pass to remove the inelastically scattered electrons and thus produce micrographs free of chromatic aberrations with elastically scattered electrons or, complementarily, (2) the filter is used to select inelastically scattered electrons within a certain energy-loss range and to record their contribution to an image (electron spectroscopic imaging) or diffraction pattern (ESD). Furthermore, the electron energy-loss spectrum (EELS) can be recorded.

However, little information is extracted from large-angle inelastic scattering of fast electrons. Electron energy loss under large scattering angle is a rather demanding field of work for a number of reasons. The main problem is the low cross section at high scattering angle that essentially precludes experiments with a *serial* spectrometer. On the other hand, these experiments would be very attractive since they directly yield the momentum density, via the Compton profiles.² Besides the experimental difficulties, calculation of the Compton profile is a demanding task for other than the simplest cases. Therefore early attempts³ were likely to fail. But nowadays, available instrumentation such as parallel EELS (PEELS) or ESD allows reasonable dwell times and considerable progress in the theoretical calculation of Compton profiles has been achieved.

It has been shown that electron Compton experiments are feasible with PEELS, yielding momentum anisotropies with equal or better resolution than the conventional Compton scattering work with photons, and on a spatial

scale of micrometers.⁴ The alternative experimental technique, ESD, has only been used to demonstrate the existence of a Compton maximum in the diffraction plane.⁵ Previous experiments did not agree on the position of this maximum. Egerton reported a constant shift of the Compton maximum with respect to the expected $E=q^2/2$ behavior,⁶ whereas Reimer *et al.*⁵ found different deviations of the maximum in $d^2\sigma/dE d\Omega$ from $E=q^2/2$ in different materials. The aim of this paper is to repeat the experiments under controlled conditions, and to give a theoretical explanation of the disagreements in previous work. This is an important step in developing a potentially powerful method of solid-state spectroscopy.

CROSS SECTION

The contrast in the micrograph (Fig. 1) taken with a modern electron microscope with an energy filter is a picture of the differential interaction cross section within the thin sample. Since the usual kinetic energy of the illuminating electrons is high compared to energy states of the solid sample, the cross section can be separated conveniently into two factors, one describing the fate of the primary electron by the Rutherford cross section and another called the dynamic structure factor, which describes the response of the sample to the transfer of a momentum \mathbf{q} and an energy E from the primary electron:

$$\frac{d^2\sigma}{dEd\Omega} = \frac{p_1}{p_f} \cdot \left[\frac{d\sigma}{d\Omega} \right]_{\text{Ruth}} \cdot S(\mathbf{q}, E). \quad (1)$$

p_i and p_f are the momenta of the primary electrons before and after scattering, respectively. We use atomic units and the formulas are dimensionless. In these units, $(d\sigma/d\Omega)_{\text{Ruth}} = 4/q^4$.

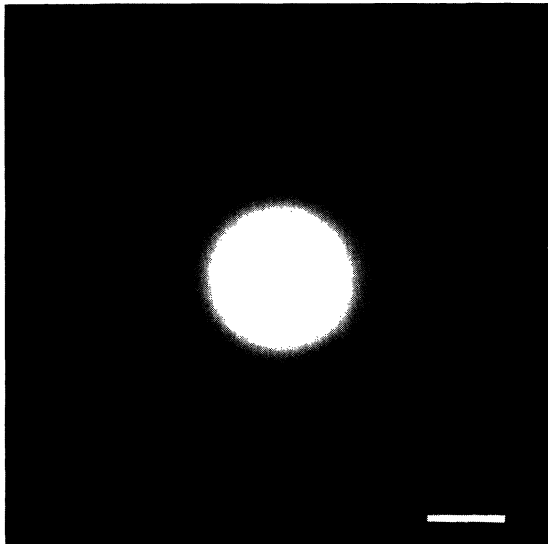


FIG. 1. ESD with $E = 500$ eV from Zeiss EM 902 on a carbon film. Scale bar in micrograph corresponds to 2 a.u.

For the microscopist only the dynamical structure factor is of interest because it relates to the materials characteristics of the sample. Depending on the experimental setting, that is, on the selection of the ranges in q and E , different responses of the target dominate. Therefore $S(\mathbf{q}, E)$ may be related to either the dielectrical function for collective excitation of valence electrons⁷ or to the generalized oscillator strength for ionization of core electrons.⁸

We are mainly interested in the inelastic scattering of fast electrons with large energy and momentum transfer to the target electron, so large that the binding energy E_B of target electrons is insignificant. The scattering can be considered as a classic binary collision of two seemingly free electrons, for which the conservation of energy and momentum leads to

$$E = \frac{q^2}{2} + \mathbf{p} \cdot \mathbf{q}, \quad (2)$$

where \mathbf{p} is the initial momentum of the target electron. The first term on the right-hand side of Eq. (2) gives the energy transfer for scattering off *stationary* free electrons and depends only on the incident energy and the scattering angle, hence the energy loss is a δ function peaking at an energy $E = q^2/2$. The second term is proportional to the projection of the initial momentum of the sample electron onto the scattering vector and broadens the energy-loss distribution of the scattered electrons (Doppler broadening). The resulting spectrum therefore provides a direct measure of the ground-state momentum distribution of the electrons in the sample.

In fact, very short-time interactions, i.e., high-energy transfer ($E \propto t^{-1}$), permit one to consider the potential experienced by the primary electron as invariant. It can be shown that the binding energy of the target electron is canceled in this so-called impulse approximation;⁹ therefore the initial ground state of the bound electrons can be

taken as one with momentum \mathbf{p} and energy $p^2/2$ (not $-E_B$), which leads to an expression for $S(q, E)$

$$S = \frac{1}{(2\pi)^2} \cdot \frac{1}{q} \cdot J(p) \quad (3)$$

with

$$p = \frac{\mathbf{p} \cdot \mathbf{q}}{q} = \frac{1}{q} \cdot \left[E - \frac{q^2}{2} \right]. \quad (4)$$

For historical reasons $J(p)$ is also called the Compton profile, being the projection integral of the three-dimensional momentum density distribution of the target electrons onto the direction of the scattering vector \mathbf{q} . The theoretical calculation and experimental determination of the Compton profile $J(p)$ constitutes a major effort in electron and synchrotron scattering experiments.

As an example one Compton profile calculated for metallic aluminum with the free-electron model for conduction electrons and with the impulse hydrogenic model¹⁰ for inner-shell electrons is shown in Fig. 2. The profile shows the two contributions distinctly separated into a flat extended region (the momentum distribution of the L -shell electrons) and a narrow parabola, superimposed. The momenta where the slope changes discontinuously designate the Fermi momentum of the conduction electrons. The profile is normalized such that the area under the parabola corresponds to 3, the number of the valence electrons, and the area under the lower portions to 10, the number of core electrons.

Equation (4) is the same as Eq. (2); in fact the impulse approximation is equivalent to the classical binary collision, and predicts that $J(p)$ (not another quantity) has a maximum at $p=0$, or at $E = q^2/2$. It has been accepted as a good approximation if the energy transfer is larger than $4E_B$.²

EXPERIMENT

We use a commercially available Zeiss EM 902 electron microscope with an integrated Castaing-Henry filter,¹¹ which consists of an electrostatic mirror and a

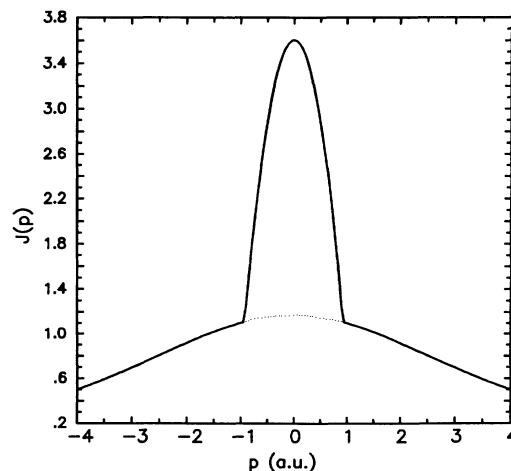


FIG. 2. The Compton profile of metallic aluminum showing the two contributions of conduction and inner-shell electrons.

magnetic prism. The primary electrons are accelerated to 80 keV and focused onto the specimen. Anticipated energy losses are compensated by adding a ramp voltage to the accelerating voltage, thus leaving the electron energies at the filter entrance constant. The energy-loss spectrum in the energy-dispersive plane of the filter is then shifted and a selecting slit on the optical axis selects electrons with the chosen energy loss. In the ESD mode, the filter entrance plane contains an electron-diffraction pattern, which is then projected onto the final viewing screen.⁵ Therefore the ESD can give the diffraction pattern of elastically scattered electrons (zero-loss filtering) or of inelastically scattered electrons with lower energy loss. With high-energy loss ESD depicts the diffuse ring of Compton-scattered electrons. Measurements were performed on C film with energy loss higher than 100 eV to avoid the possible influence of the amorphous rings and on Al film with energy loss higher than 400 eV so that the binary collision condition is fulfilled. The intensities are recorded on a photographic plate with exposure times from 50 to 500 s depending on the energy loss.

For an energy loss E the energy resolution needed to achieve a given momentum resolution δp is $\delta E = \delta p \cdot (2E)^{1/2}$. Using a selecting slit δE of 5 eV for an energy transfer of, say, 230 eV, a momentum resolution of 0.04 a.u. is easily achieved. For high-energy transfer, a slightly wider slit may be used to gain more intensity without loss of the momentum resolution. This momentum resolution is about half of the best resolution that one may achieve with a synchrotron experiment for which counting times of hours or days may be needed. However, the real momentum resolution is worse than this ideal value due to the compromise necessary between a tolerable divergence and a useful intensity of the beam through the angle-limiting narrow condenser aperture.⁴ By this the illumination angle is limited to 0.6 mrad and the final momentum transfer uncertainty amounts to ~ 0.06 a.u.

Due to the second-order aberrations of the Castaing-Henry filter, the image details located at a certain distance off the optic axis are related to smaller energy losses than those on axis. For ESD with an energy loss of 230 eV on axis, for instance, the energy loss on the final viewing screen 2 cm off axis is 226 eV; the resulting momentum uncertainty is less than 0.06 a.u.

Thin films of carbon were prepared by vacuum deposition onto a clean mica surface and subsequent floating off in distilled water. For the metallic films aluminum was evaporated from a tungsten boat onto a glass surface covered with Movital for easy removal. Electron-diffraction patterns confirmed the amorphous character of the C films and the polycrystalline structure of the Al films: They showed three broad rings in the first case and spotted Debye-Scherrer rings in the second.

The experimental results were obtained by densitometry of photoplates, whereby the Debye-Scherrer rings of the Al film was used for calibrating the q scale.

RESULTS AND DISCUSSION

Before interpreting these findings in terms of electron Compton scattering, it must be assured that they are not

disturbed by multiple scattering of incident electrons. A simulation study shows that for high-energy losses small scattering angle events do not mix significantly with the Compton scattering.¹² For example, in an Al film of 20 nm corresponding to 20% of the mean free path for plasmons, the amount of combined plasmon-Compton scattering is less than 20% and does *not* displace the maximum position of the final intensity distribution.¹³ The mixed elastic/inelastic-scattering results in the background which decreases monotonically with increasing energy loss and scattering angle. For this case the simulations show a slight downward shift of the maximum, which, however, is smaller than the instrumental resolution (for a thickness of about 20% of the mean free path for plasmons). Therefore we feel justified in neglecting the influence of multiple scattering in the chosen angular and energy region.

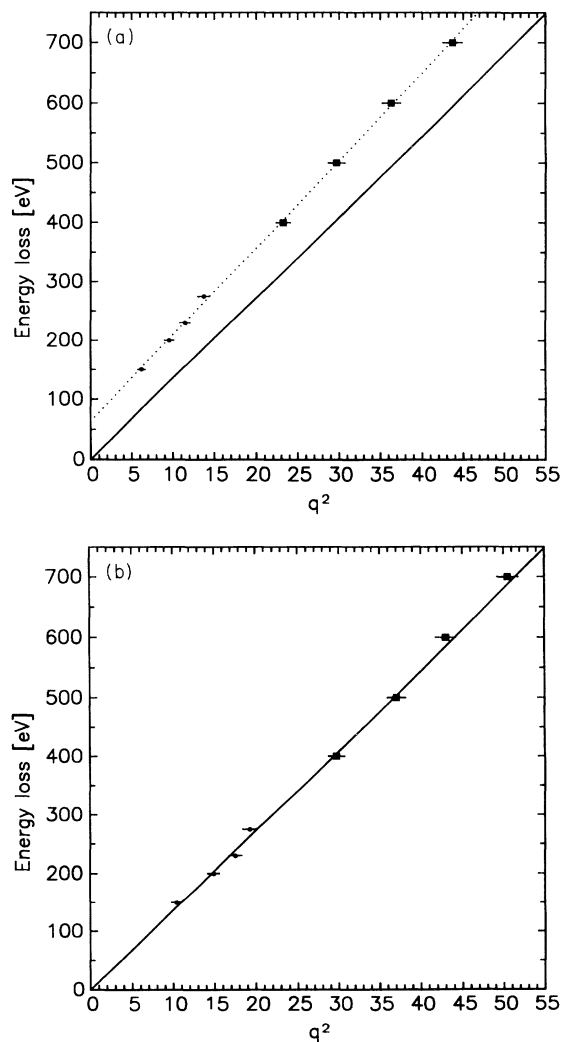


FIG. 3. (a) Maximum positions in $d^2\sigma/dE d\Omega$; (b) maximum positions in Compton profile $J(p)$. ●: amorphous carbon; ■: polycrystalline Al; the solid line is the prediction of binary collision mode, the dotted line is the fitting of the experimental results. The error bars reflect the uncertainty in the beam momentum and the spot size of the densitometer.

We discuss first the dependence of the maximum in differential cross section $d^2\sigma/dEd\Omega$ on momentum transfer q . The energy dispersion of this maximum is shown in Fig. 3(a) for the energy region 150–280 eV for carbon and 500–700 eV for metallic Al. The inelastic scattering in carbon is only due to the excitation of the valence electrons because the energy losses are less than the threshold of K -shell electrons. In Al the valence and L -shell electrons will be excited. For losses E much higher than the Fermi energy and fulfilling the binary collision condition for L electrons, we find a quadratic relation between energy and momentum independent of the atomic number Z ; it can be approximated as

$$E = A + \frac{\alpha}{2}q^2 \quad (5)$$

with $A = 2.3$ (63 eV) and $\alpha = 1.07$. Since the results are independent of atomic number, we may conclude the binary collision property of the electron scattering in the solid. However, the existence of a threshold ($A \neq 0$) and the deviation of α from unity refutes the notion of free collision partners.

Our carbon results can be compared with those of Egerton.⁶ Egerton gave the position of the peak approximately by $E = E_1 + E_0 \cdot \theta^2$, with $E_1 = 80$ eV. This is a constant shift from the prediction of the binary collision model giving the scattering angle $\theta^2 = E/E_0$. In our experiments $E_1 = 63$ eV, less than the value from Egerton,

and the shift increases as E increases, reflected by $\alpha \neq 1$ in Eq. (5). It has been concluded that this model is not suitable for the case of solids.⁶

As shown above, however, the reason for this discrepancy is that only the Compton profile $J(p)$ has its maximum at $E = q^2/2$, whereas the measured cross section $d^2\sigma/dEd\Omega$ has not. This is perfectly verified by the present experiment, shown in Fig. 3(b). Only in case of target electrons at rest would the two maxima coincide since $J(p) \propto \delta(p)$.

CONCLUSION

The angular dependence of the Rutherford differential cross section causes the maximum position of the electron Compton scattering to deviate by a nearly constant amount from the position $E = q^2/2$, expected from the theory. These findings are independent of the atomic number. The maximum position of the experimental Compton profile agrees perfectly with the prediction of the impulse approximation.

ACKNOWLEDGMENTS

We thank S. Subramanian and M. Swoboda for supporting experiments. D. S. S. gratefully acknowledges financial support by the Max Planck Society and P. S. financial support of the Hochschuljubiläumsstiftung der Stadt Wien.

¹J. Mayer, *Eur. Microscopy Anal.* **25**, 21 (1993).

²B. G. Williams, *Compton Scattering* (McGraw-Hill, New York, 1977).

³B. G. Williams, G. M. Parkinson, C. J. Eckhardt, J. M. Thomas, and T. G. Sparrow, *Chem. Phys. Lett.* **78**, 434 (1981).

⁴P. Jonas and P. Schattschneider, *J. Phys. Condens. Matter* **5**, 7173 (1993).

⁵L. Reimer, I. Fromm, C. Hülk, and R. Rennekamp, *Microsc. Microanal. Microstruct.* **3**, 141 (1992).

⁶R. F. Egerton, *Philos. Mag.* **31**, 199 (1975).

⁷D. Pines, *Elementary Excitations in Solids* (Benjamin, New York, 1964).

⁸M. Inokuti, *Rev. Mod. Phys.* **43**, 297 (1971).

⁹P. Schattschneider, *Scanning Microsc. Suppl.* **4**, 35 (1990).

¹⁰B. J. Bloch and L. B. Mendelsohn, *Phys. Rev.* **9**, 129 (1974).

¹¹R. Castaing and L. Henry, *C. R. Acad. Sci.* **255**, 76 (1962).

¹²D. S. Su and E. Zeitler, *Phys. Rev. B* **47**, 14 734 (1993).

¹³D. S. Su, P. Jonas, and P. Schattschneider, *Philos. Mag. B* **66**, 405 (1992).

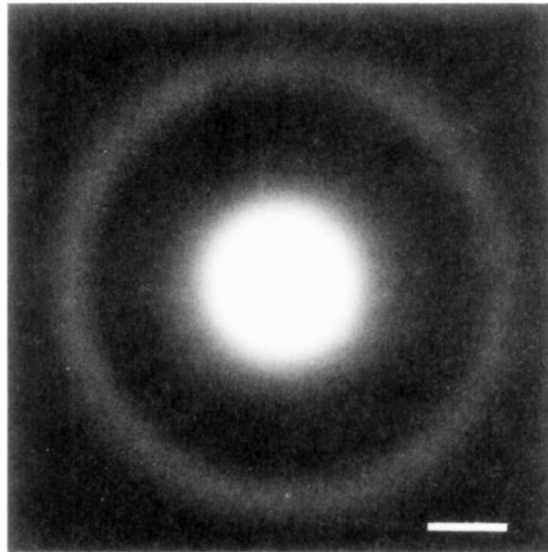


FIG. 1. ESD with $E = 500$ eV from Zeiss EM 902 on a carbon film. Scale bar in micrograph corresponds to 2 a.u.